Quantitative measurement of local elasticity of SiO_x film by atomic force acoustic microscopy*

He Cun-Fu(何存富)†, Zhang Gai-Mei(张改梅), and Wu Bin(吴 斌)

College of Mechanical Engineering & Applied Electronics Technology, Beijing University of Technology, Beijing 100124, *China*

(Received 5 August 2009; revised manuscript received 24 January 2010)

In this paper the elastic properties of SiO_x film are investigated quantitatively for local fixed point and qualitatively for overall area by atomic force acoustic microscopy (AFAM) in which the sample is vibrated at the ultrasonic frequency while the sample surface is touched and scanned with the tip contacting the sample respectively for fixed point and continuous measurements. The SiO_x films on the silicon wafers are prepared by the plasma enhanced chemical vapour deposition (PECVD). The local contact stiffness of the tip-SiO_x film is calculated from the contact resonance spectrum measured with the atomic force acoustic microscopy. Using the reference approach, indentation modulus of SiO_x film for fixed point is obtained. The images of cantilever amplitude are also visualized and analysed when the SiO_x surface is excited at a fixed frequency. The results show that the acoustic amplitude images can reflect the elastic properties of the sample.

Keywords: atomic force acoustic microscopy, SiO_x film, contact resonance frequency, local elasticity

PACC: 4385G, 5360, 8170G

1. Introduction

The wide application of the nanoscale materials, devices and systems requires the exact knowledge and the control of material properties on an ultra-small scale. It is obviously more desirable to directly probe the local mechanical properties of a nanostructured material.[1] Many static and dynamic methods to measure small-scale mechanical properties have been devised. The static methods include force-distance method with atomic force microscope (AFM)[2,3] and nanoindentation tests.[4−6] The force-distance method works best when the compliance of the cantilever is roughly comparable to that of the test material. Therefore it is better suited to very compliant material, and loses the effectiveness as the material stiffness increases. The nanoindentation is inherently destructive and the lateral resolution is about a few hundred nanometers. To meet the requirements for non-destruction and high resolution, researchers developed a dynamic technique combining contact-resonance atomic force microscopy with acoustic excitation technique to determine the elastic modulus of material with nanoscale features, called atomic force acoustic microscopy (AFAM).[7−10] The AFM cantilever or the sample surface is vibrated at an ultrasonic frequency while a sample surface is scanned with the sensor tip contacting the sample. As a consequence, the amplitude of the vibration of the cantilever as well as the shift of the cantilever resonance frequencies contain information about the local tip-sample contact stiffness and can be used for imaging quantitatively. The AFAM images of the piezoelectric lead zirconate ceramic had been shown.[9] The local elastic properties of ferroelectric domain configuration have been examined by atomic force acoustic microscopy.[10−12] In the present work, the SiO_x films are prepared by the plasma enhanced chemical vapour deposition (PECVD) and a custom-made AFAM was developed in our laboratory. From the measured tip-sample contact resonance frequencies and free resonance frequencies of the cantilever, we can deduce the local elastic modulus of the sample for fixed point. Also, we can obtain the acoustic amplitude image of the sample, which can reflect the local elasticity for certain areas. Meanwhile, the acoustic amplitude images are explained by the repulsion force and the contact stiffness between the tip and the sample during

*Project supported by the National Natural Science Foundation of China (Grant No. 50775005).

†Corresponding author. E-mail: hecunfu@hotmail.com, hecunfu@bjut.edu.cn

© 2010 Chinese Physical Society and IOP Publishing Ltd

scanning.

2. Experiment

2.1. Sample preparation

The single crystal silicon (111) wafers serving as the substrates were cleaned sequentially in an ultrasonic bath using ethanol, acetone and de-ionized water before they were mounted on the sample holder. Hexamethyldisiloxane (HMDSO) in mixture with oxygen (O_2) was used as deposition gases. The SiO_x films were deposited by PECVD through glow discharge. The background pressure was 4.1 Pa, oxygen flow rate was 21 sccm, monomer flow rate was 10.5 sccm, and input power was kept at 200 W for 20 min during the deposition. The thicknesses of the silicon wafer and SiO_x coating were 0.5 mm and 110 nm respectively.

2.2. AFAM experimental setup

A modified commercial atomic force microscope is used to image the sample surface, and to control the static cantilever forces before the tip contacts the sample. Table 1 shows the parameters of nominal length L, width W, thickness t and spring constant k_c of the cantilever, given by the manufacturer. An external function generator (Handyscope-HS3, TiePie, UK) provides a stable sinusoidal excitation, which is applied to a piezoelectric transducer (V103-RM, Panametrics, USA) coupled to the back side of the sample with the double-sided tape as shown in Figs. 1 and 2. Figures 1 and 2 show the block diagram and actual photograph of the AFAM system. The transducer, working in the thickness vibration mode, sends longitudinal acoustic waves into the sample, which causes out-of-plane vibration of the sample surface. These surface vibrations are transmitted into the cantilever via the sensor tip. The cantilever vibrations are measured by the photodiode detector of the AFM instrument, and the signal is transmitted to the signal channel of lock-in amplifier (Model 7280 DSP, Signal Recovery, USA) which also receives a reference signal from the function generator in the reference channel.

Table 1. Parameters of the AFM cantilever provided by manufacturer.

parameters	L/μm	W/μm	t/μm	$k_c/\mathrm{N\cdot m^{-1}}$
nominal value	225	38	7	48

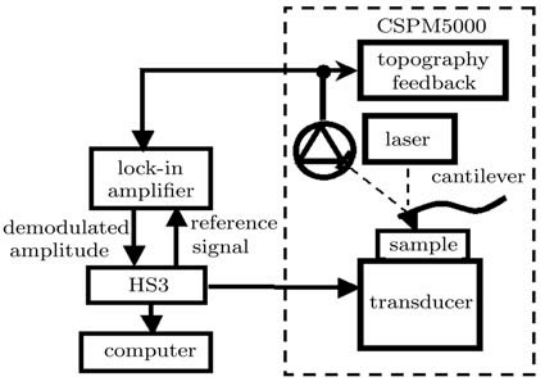


Fig. 1. Block diagram of AFAM system.

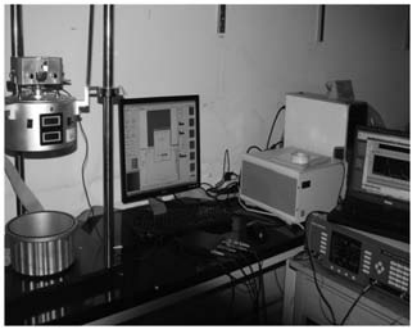
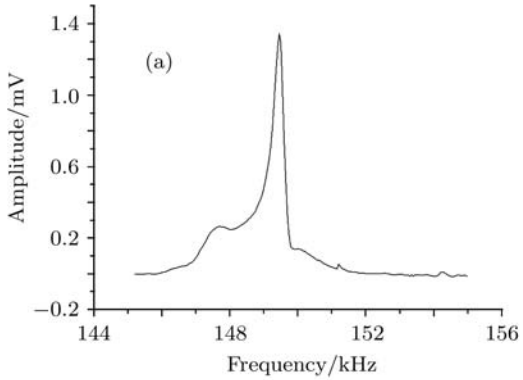


Fig. 2. Photograph of AFAM system.

2.3. Data acquisition

To measure the contact resonance frequencies for the fixed point of sample, the amplitude of the cantilever vibration is demodulated by the lock-in amplifier only at an excitation frequency and is output to HS3. The data acquisition software is available from the commercial tool Labview (National Instruments Corp., Austin, TX), by which the excitation frequency is changed stepwise and the digitized lock-in output at the specific frequency is read. And the amplitude of the cantilever versus excitation frequency is stored and shown in Fig. 3. For imaging, a fixed



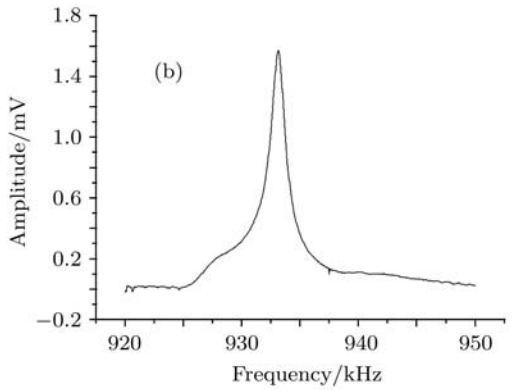


Fig. 3. The first order (a) and second order (b) free flexural resonance spectra of the cantilever beam.

excitation frequency is selected. While the sample surface is scanned, the amplitude of the cantilever is output into an auxiliary channel of the AFM and is imaged.

3. Results

3.1. Measurement of free resonance frequency

Before performing contact experiment, the free (natural) frequencies of the cantilever must be measured when the tip is out of contact.[1] The cantilever is brought close to, but it is not in contact with, the specimen. The actuator driven at a relatively high voltage creates acoustic vibrations, which are large enough to excite the free resonances of the cantilever via air coupling. The free resonance spectra are shown in Figs. 3(a) and 3(b), displaying the first and second order resonance frequencies respectively. The measured data are shown in Table 2, where f_1^0 and f_2^0 are the first and second free resonance frequencies respectively and the theoretical value of the f_2^0/f_1^0 is obtained from the analytical model, and can be seen in Eq. (2) in Section 4.

Table 2. Data measured by AFAM.

f_1^0/kHz	f_2^0/kHz	f_2^0/f_1^0	theory (f_2^0/f_1^0)
149.6	933.1	6.237	6.258

3.2. Contact resonance spectra of Si and SiO_x

In order to measure the test sample, a reference or comparison approach is used,[9,10] in which measurements are performed on the test sample and the reference sample under the same static forces separately. Using Si as a reference sample, the contact resonance spectrum measured on the Si is shown in Fig. 4(a), while the contact resonance spectrum measured on the test sample, the SiO_x film obtained by the PECVD, is shown in Fig. 4(b). From Fig. 4, it can be seen that the first and second contact resonance frequencies are clearly visible in the spectra, indicating that the first and second contact resonance frequencies are $f_1 = 650$ kHz and $f_2 = 1.450$ MHz for Si and $f_1 = 645$ kHz and $f_2 = 1.295$ MHz for SiO_x film respectively.

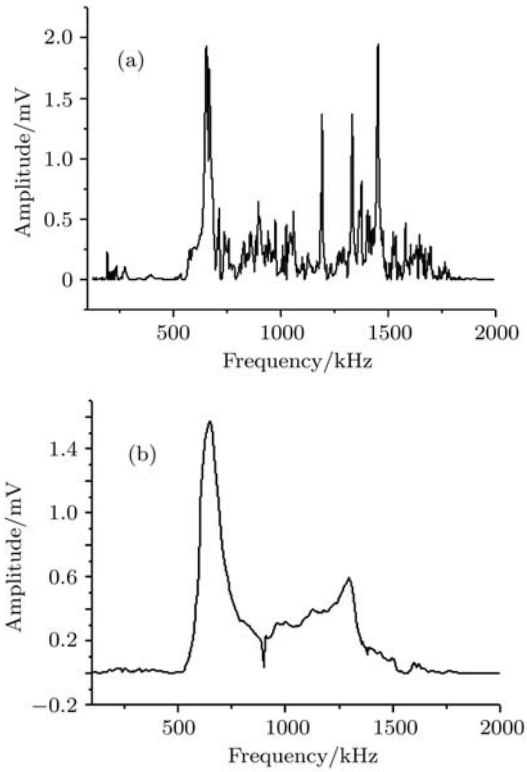


Fig. 4. Contact resonance spectra of the first and second modes for Si(111) substrate (a) and SiO_x film (b).

4. Analysis and discussion

4.1. Analysis method

If the tip and the sample vibration amplitudes are kept sufficiently small, the tip-sample forces can be approximated by linear vertical spring dashpot systems. A simplified model is shown in Fig. 5,[7] where k_s is the tip-sample contact stiffness, L is the total length of the cantilever, L_1 is the length between the tip and the cantilever base, L_2 is the distance between the tip base and the end of the cantilever.

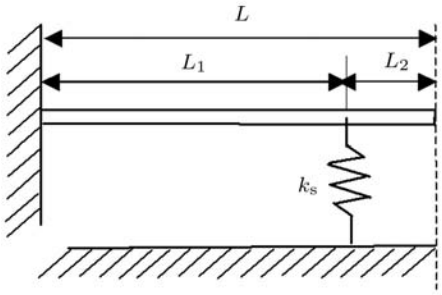


Fig. 5. Flexural beam model for the AFM cantilever with sensor tip.

The characteristic equation of the simplified system shown in Fig. 5 is given as follows:

$$\begin{aligned}&\frac{k_{\rm s}}{k_{\rm c}}\{-(\cosh k_n\ L_1\sin k_nL_1-\sinh k_nL_1\cos k_nL_1)\\&\times(1+\cos k_nL_2\cosh k_nL_2)\\&+(\cosh k_nL_2\sin k_nL_2-\sinh k_nL_2\cos k_nL_2)\\&\times(1-\cos k_nL_1\cosh k_nL_1)\}\\&=\frac{2(k_nL_1)^3}{3}(1+\cos k_nL\cosh k_nL),\end{aligned}\tag{1}$$

where k_n is the wavevector of the n-th eigen-mode of the AFM cantilever.

Like macroscopic beams, the AFM cantilevers can vibrate in the different types of acoustic modes, such as flexural, torsional or extensional modes. The resonance frequencies for flexural vibration are related to wave number by

$$k_nL=c_{\rm B}L\sqrt{f_n}\quad n=1,2,3,4\ldots,\tag{2}$$

where $c_{\rm B}$ is a characteristic cantilever constant containing Young's modulus E, mass density ρ of the cantilever material, and thickness t of the beam; f_n is the free resonance frequency.

If the tip is far from the sample surface, contact stiffness $k_{\rm s}$ is zero and equation (1) reduces into the characteristic equation for free flexural vibrations of the cantilever, given as

$$(1+\cos k_nL\cosh k_nL)=0.\tag{3}$$

The solutions of Eq. (3) for the different vibration modes n are known to be $k_1L=1.8751$, $k_2L=4.69409$, $k_3L=7.85476$, $\ldots,n=1,2,3,4\ldots$. By measuring the free resonance frequencies and substituting the measured values into Eq. (2), $c_{\rm B}L$ can be determined in a high accuracy and without the knowledge of any additional cantilever data. To solve equation for $k_{\rm s}$, not only the $c_{\rm B}L$ but also the relative tip position $c_{\rm B}L_1$ is needed. The unknown second parameter L_1 can be determined from Eq. (1) itself by using its dispersive behaviour. The values of contact stiffness $k_{\rm s}$ must be the same for all cantilever modes for a given measurement. We determine the eigenfrequencies of the first two modes, and calculate $c_{\rm B}L$ and vary the ratio L_1/L in a range which is reasonable compared with the micrographs. The contact stiffness $k_{\rm s}$ obtained from Eq. (1) is plotted as a function of the value of L_1/L for the first two modes. The values of resulting contact stiffness $k_{\rm s}$ must be the same for all cantilever modes when the same static tip-sample forces are maintained. According to the Hertz model we can obtain

$$k_{\rm s}=\sqrt[3]{6E^{*2}RF_0},\tag{4}$$

where E^* is the effective Yong's modulus of the tip-sample contact; F_0 is the normal force acting on the tip. We also have

$$E^*=\left(\frac{1}{M_{\rm s}}+\frac{1}{M_t}\right)^{-1},\tag{5}$$

where $M_{\rm t}$ and $M_{\rm s}$ are the indentation moduli of the tip and the sample, respectively.

4.2. Calculation of elasticity of test sample for fixed point

As mentioned before, the reference sample is Si, so the value of $M_{\rm ref}$ and thus the value of $E^*_{\rm ref}$ are known. According to the Hertzian contact, the following relationship can be obtained:

$$E^*_{\rm s}=E^*_{\rm ref}\left(\frac{k_{\rm s}}{k_{\rm ref}}\right)^{3/2}.\tag{6}$$

In order to use the reference approach, we set the cantilever static deflection $d=10$ nm ($F_0=480$ nN). According to the contact resonance frequencies of the reference sample and the test sample, we can obtain the relationships between L_1/L and contact stiffness $k_{\rm s}$ of the tip-Si and the tip-SiO_x as shown in Figs. 6(a) and 6(b).

From Figs. 6(a) and 6(b), we can obtain $L_1/L=0.953$ and $k_{\rm ref}=2368$ N/m for the Si reference sample and $L_1/L=0.935$ and $k_{\rm s}=1750$ N/m for the test sample SiO_x. Assuming $M_{\rm tip}=165.5$ GPa and $M_{\rm ref}=175$ GPa,[10] we can obtain $E^*_{\rm ref}=85.06$ GPa. From Eqs. (6) and (5) it follows that $E^*=54.04$ GPa and $M_{SiO_x}=78.18$ GPa. The measured values are in agreement with the values for bulk fused silica ($M_{SiO_2}=72\sim77$ GPa).

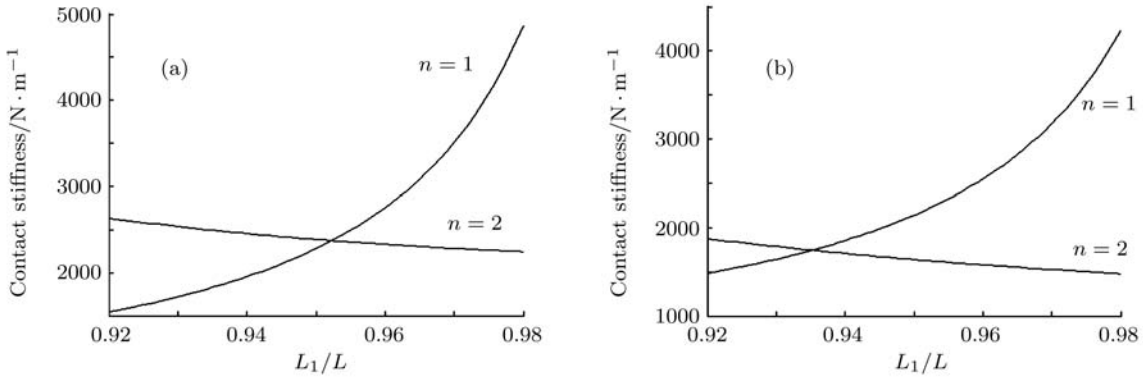


Fig. 6. Contact stiffnesses as a function of relative tip position L_1/L for Si as reference sample (a) and SiO_x film as test sample (b).

4.3. Analysis of acoustic amplitude images

4.3.1. Contact resonance spectra under different static forces for SiO_x surface

According to Eqs. (5) and (4), we can find that the contact stiffness will increase with the increase of static force F_0 or the elastic modulus of sample surface M_s. From Eq. (1), we can know that the contact resonance frequency increases with contact stiffness increasing. Using the same type of cantilever as that in Table 1, we can obtain the first contact resonance spectra of SiO_x with different values of F_0 as shown in Fig. 7. The results show that the contact resonance frequency and the amplitude increase with the value of F_0 increasing. From Fig. 7, different values of F_0 will induce different contact resonance frequencies even for the same fixed point of the sample. And the contact resonance frequency is 675 kHz for a 480-nN static force.

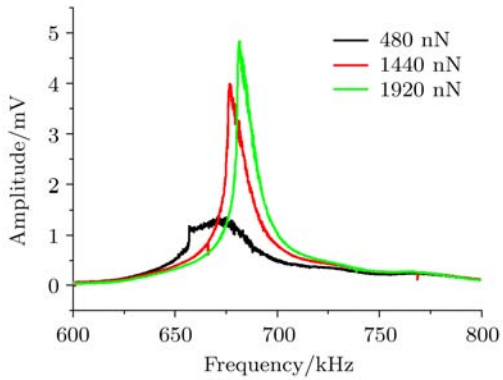
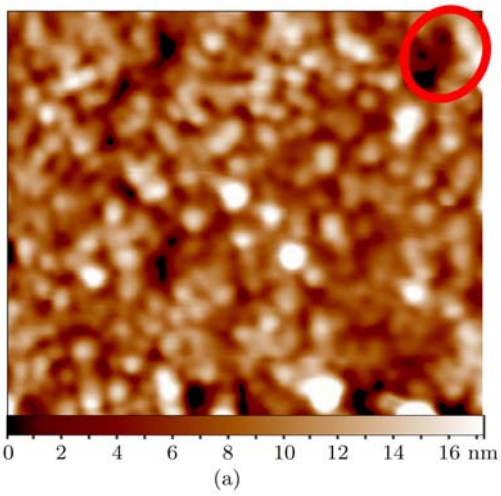


Fig. 7. The first order resonance frequencies of SiO_x film under different values of F_0.

4.3.2. Analysis of acoustic amplitude images

4.3.2.1. Experimental results of acoustic amplitude images

Under the same static force $F_0 = 480$ nN, we scan the SiO_x surface excited by the signal with different frequencies and the same amplitude ($V_{p-p} = 2$ V). We can obtain the topography image and the acoustic amplitude images of the same area (5 μm×5 μm) vibrated at different excitation frequencies as given in Fig. 8. When the excitation frequency is 650 kHz, which is below the contact resonance frequency, the contrast of the two images is inverse in brightness as shown in Fig. 8(a) for the topography and Fig. 8(b) for acoustic amplitude images in ellipse regions. When the excitation frequency is 700 kHz, which is above the contact resonance frequency, the contrast in brightness between the two images is consistent with that between the images in Figs. 9(a) and 9(b). When



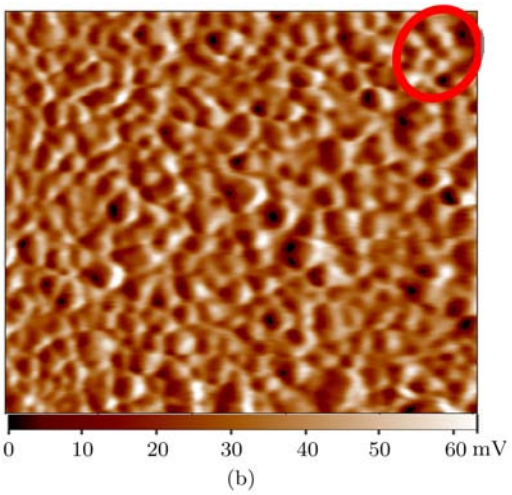


Fig. 8. Topography (a) and acoustic amplitude (b) images of SiO_x film excited at 650 kHz.

the excitation frequency is far from the contact resonance frequency, such as 900 kHz, the amplitude of the cantilever becomes smaller as shown in Fig. 10(b) for acoustic amplitude images, in which the contrast of amplitude reduces.

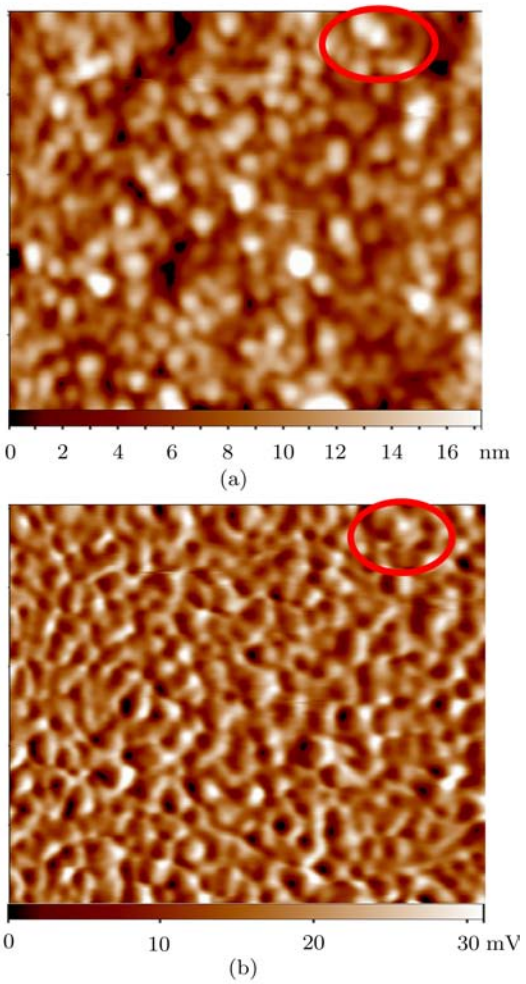


Fig. 9. Topography (a) and acoustic amplitude (b) images of SiO_x film excited at 700 kHz.

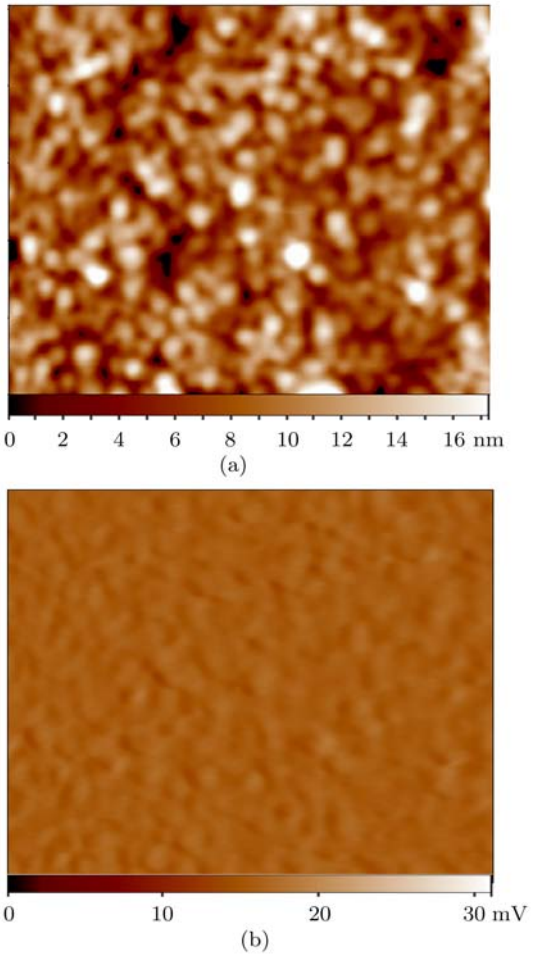


Fig. 10. Topography (a) and acoustic amplitude (b) images of SiO_x film excited at 900 kHz.

4.3.2.2. Analysis of acoustic amplitude images

In the acoustic amplitude images, the amplitude contrasts reflect the responses of SiO_x film to the local elastic displacement fields in the sample, which is closely relevant to the local contact stiffness between the tip and the sample surface during scanning. The surface with higher elastic modulus, called as stiff surface, generates contact resonance curves with increased central frequency and higher amplitude than the surface with lower elastic modulus, called as soft surface.[13,14] The vibration frequency spectra of the tip (cantilever) for different contact stiffness are shown schematically in Fig. 11.

In topography images, dark regions indicate lower morphology and brighter regions represent higher one. In the acoustic amplitude images, the amplitudes are higher in brighter regions and smaller in darker regions. When the tip scans the lower surface of the topography image, the tip-sample repulsion is smaller. Equivalently, the contact stiffness is smaller in the

lower surface of the topography than in higher surface of the topography. So, when the excitation frequency is near the contact resonance frequency of the

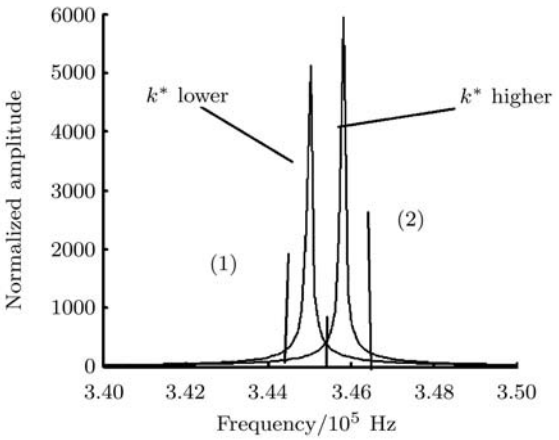


Fig. 11. Vibration frequency spectra of the tip (cantilever) for different contact stiffness.

darker area (equal to soft surface area), the cantilever acoustic amplitude is higher in the soft area, the contrast in brightness between the topography image and the acoustic amplitude image is inverse, which can be seen in Fig. 8. When the excitation frequency is near the contact resonance frequency of the brighter area (equal to stiff surface area) of the topography, the cantilever acoustic amplitude is higher in the stiff area, the contrast in brightness between the topography image and the acoustic amplitude image is consistent, which can be seen in Fig. 9. But when the excitation frequency is far from the contact resonance frequency and the excitation amplitude is not high enough, the cantilever acoustic amplitude is very low both in the stiff area and the soft areas so the contrast in brightness is small as shown in Fig. 10(b). From Figs. 8(a), 9(a) and 10(a), we can find that they are identical except for the drift during the scanning and only contain the information about topography. But in acoustic amplitude images, they vary with excitation frequency and the contrast in brightness can qualitatively reflect elastic property.

5. Conclusion

The results show that the AFAM technique is a sensitive method of quantitatively measuring the indentation modulus for fixed point. Experimentally, quantitative results on SiO_x film are presented, and they are in agreement with the values for bulk fused silica. The acoustic amplitude has been exploited to image, which can reflect the local elasticity qualitatively. The acoustic amplitude images are different when the sample is excited with the different frequencies. The quantitative elastic modulus images will be studied for SiO_x film in future work.

Acknowledgement

We thank Chen Qiang, the Laboratory of Plasma Physics and Materials, Beijing Institute of Graphic Communication, for the preparation of the SiO_x films and the helpful discussions.

References

[1] Hurley D C 2008 *Applied Scanning Probe Methods* XI (Berlin, Heidelberg: Springer-Verlag) p. 98
[2] Cappella B and Dietler G 1999 *Surf. Sci. Rep.* **34** 1
[3] Zhong Q, Inniss D, Kjoller K and Elings V B 1993 *Surf. Sci.* **290** L688
[4] Oliver W C and Pharr G M 1992 *J. Mater. Res.* **7** 1564
[5] Syed Asif S A, Wahl K J, Colton R J and Warren O L 2001 *J. Appl. Phys.* **90** 5838
[6] Li X D and Bhushan B 2002 *Materials Characterization* **48** 11
[7] Rabe U, Janser J and Arnold W 1996 *Rev. Sci. Instrum.* **67** 3281
[8] Passeri D, Bettucci A, Germano M, Rossi M, Alippi A, Orlanducci S, Terranova M L and Ciavarella M 2005 *Rev. Sci. Instrum.* **76** 093904
[9] Hurley D C, Shen K, Jennett N M and Turner J A 2003 *J. Appl. Phys.* **94** 2347
[10] Rabe U, Amelio S, Kopycinska M, Hirsekorn S, Kempf M, Göken M and Arnold W 2002 *Surf. Interface Anal.* **33** 65
[11] Zeng H R, Yu H F, Hui S X, Chu R Q, Li G R, Luo H S and Yin Q R 2005 *Solid State Commun.* **133** 521
[12] Zhao K Y, Zeng H R, Song H Z, Hui S X, Li G R, Yin Q R, Shimamura K, Kanna C V, Villora E A G, Takekawa S and Kitamura K 2008 *Chin. PJYS. Lett.* **25** 3429
[13] Rabe U, Amelio S, Kester E, Scherer V, Hirsekorn S and Arnold W 2000 *Ultrasonics* **38** 430
[14] Amelio S, Goldade A V, Rabe U, Scherer V, Bhushan B and Arnold W 2001 *Thin Solid Films* **392** 75